ISSN 1674-1056
http://cpb.iphy.ac.cn
http://iopscience.iop.org/cpb
中国物理 B
Chinese Physics
中国物理 Chinese Physics B

Topological properties in ABA trilayer graphene under the irradiation of light

Liang Chen(陈亮)

Citation: Chin. Phys. B . 2019, 28(11): 117304 . **doi:** 10.1088/1674-1056/28/11/117304
Journal homepage: http://cpb.iphy.ac.cn; http://iopscience.iop.org/cpb

What follows is a list of articles you may be interested in

Adsorptions of metal adatoms on graphene-like BC_3 and their rich electronic properties: A first-principles study

Pengfei Sui(隋鹏飞), Jiaqi Dai(戴佳琦), Yinchang Zhao(赵银昌), Zhenhong Dai(戴振宏)
Chin. Phys. B . 2018, 27(9): 097311 . **doi:** 10.1088/1674-1056/27/9/097311

Highly stable two-dimensional graphene oxide: Electronic properties of its periodic structure and optical properties of its nanostructures

Qin Zhang(张琴), Hong Zhang(张红), Xin-Lu Cheng(程新路)
Chin. Phys. B . 2018, 27(2): 027301 . **doi:** 10.1088/1674-1056/27/2/027301

One-dimensional method of investigating the localized states in armchair graphene-like nanoribbons with defects

Yang Xie(谢阳), Zhi-Jian Hu(胡智健), Wen-Hao Ding(丁文浩), Xiao-Long Lü(吕小龙), Hang Xie(谢航)
Chin. Phys. B . 2017, 26(12): 127310 . **doi:** 10.1088/1674-1056/26/12/127310

Quantum spin Hall and quantum valley Hall effects in trilayer graphene and their topological structures

Majeed Ur Rehman, A A Abid
Chin. Phys. B . 2017, 26(12): 127304 . **doi:** 10.1088/1674-1056/26/12/127304

Topological transport in Dirac electronic systems: A concise review

Hua-Ding Song(宋化鼎), Dian Sheng(盛典), An-Qi Wang(王安琦), Jin-Guang Li(李金光), Da-Peng Yu(俞大鹏), Zhi-Min Liao(廖志敏)
Chin. Phys. B . 2017, 26(3): 037301 . **doi:** 10.1088/1674-1056/26/3/037301

Topological properties in ABA trilayer graphene under the irradiation of light*

Liang Chen(陈亮)†

School of Physics and Electronic Engineering, Taishan University, Taian 271000, *China*

(Received 17 June 2019; revised manuscript received 6 September 2019; published online 23 October 2019)

We study ABA trilayer graphene under irradiation of a circularly polarized light. In high-frequency regime, the effective low-energy Hamiltonian is obtained based on the Floquet theory. With increasing circularly polarized light intensity, the band structure shows a band gap closing and reopening, which happen twice. The process of the band gap closing and reopening is accompanied with a topological phase transition. We investigate the Chern numbers and the anomalous Hall conductivities to confirm the topological phase transition. The interplay between light-induced circularity-dependent effective potential and effective sublattice potential is discussed.

Keywords: graphene, light, Flouqet theory, Hall

PACS: 73.43.–f, 78.67.–n, 85.60.–q **DOI:** 10.1088/1674-1056/ab478e

1. Introduction

Graphene has attracted a great deal of attention for its unique and promising electronic properties since it was discovered experimentally in 2004.[1,2] Graphene is an allotrope of carbon in the form of a two-dimensional, atomic-scale, and hexagonal lattice. These properties enable researchers to realize electronic devices with novel quantum properties. In recent years, great theoretical and experimental research interests have been focused on multilayer graphene systems. Different from the monolayer graphene, the electronic and transport properties of multilayer graphene can be modified and tuned by changing the number of layers of graphene and stacking order in a system. Among the family of multilayer graphene, the trilayer graphene has drawn intensive research interests due to its intriguing band dispersion. Recently, experimental developments in trilayer graphene have been reported.[3–7] Experimental and theoretical researches have shown that trilayer graphene has a very high mobility, and exhibits quantum Hall effect. Scherer *et al.*[8] have shown that quantum spin Hall state can occur in interacting trilayer honeycomb lattices. Zhang *et al.*[9] observed the predicted unconventional sequence of quantum Hall effect plateaux in trilayer graphene. Anomalous and spin Hall states were studied in weakly disordered ABC-stacked trilayer graphene.[10] Using high-magnetic fields, Kumar *et al.*[11] observed compelling evidence of the integer quantum Hall effect in trilayer graphene. When interlayer displacement is zero, fractional quantum Hall states at filling factors $2/3$ and $-11/3$ were observed in BN-encapsulated trilayer graphene.[12] Barlas[13] predicted the fractional parity Hall states in trilayer graphene with mirror symmetry. When the degeneracy of the bands is lifted by Coulomb interactions, topological bands in trilayer graphene can lead to anomalous quantum Hall phases.[14]

On the other hand, achievements in laser technology and microwave techniques have made possible manipulation of quantum systems with a high-frequency electromagnetic field to explore Hall effect, which is based on the Floquet theory of periodically driven quantum systems. Particularly, electronic and transport properties of graphene are currently in the focus of attention in condensed matter physics.[15–21] However, quantum Hall phases in trilayer graphene exposed to a circularly polarized light have not been extensively and deeply studied so far. Trilayer graphene has two natural stable allotropes: (1) ABA (Bernal stacking), where the atoms of the topmost layer lie exactly on top of those of the bottom layer; (2) ABC (rhombohedral stacking), where one sublattice of the top layer lies above the center of the hexagons in the bottom layer.[22,23] In this paper, we use the Floquet theory to analyze the effect of circularly polarized light on topological properties of ABA trilayer graphene in a high-frequency limit.

The paper is organized as follows. In Section 2, we present a brief account of ABA-stacked trilayer graphene irradiated by a circularly polarized light by the Floquet theory. The band structure of the irradiated trilayer graphene are studied. In Section 3, the Hall conductivities in the irradiated trilayer graphene and corresponding Chern numbers are studied. Conclusions are given in Section 4.

2. Model, method, and band structure

The effective low-energy Hamiltonian of ABA trilayer graphene can be written as[13,24]

$$\hat{H} = \begin{pmatrix} \hat{H}_{\rm slg} & 0 \\ 0 & \hat{H}_{\rm blg} \end{pmatrix}, \tag{1}$$

*Project supported by the National Natural Science Foundation of China (Grant No. 61604106) and Shandong Provincial Natural Science Foundation, China (Grant No. ZR2014FL025).

†Corresponding author. E-mail: 30750574@163.com

© 2019 Chinese Physical Society and IOP Publishing Ltd

where we only consider the nearest intra-layer hopping an nearest inter-layer. The Hamiltonian in monolayer-like and bilayer-like blocks are defined as

$$\hat{H}_{\rm slg} = \hbar v\,(k_x\hat{\sigma}_x+\tau k_y\hat{\sigma}_y)+m_s\hat{\sigma}_z, \tag{2}$$

$$\hat{H}_{\rm blg} = -\frac{\hbar^2v^2}{\sqrt{2}\gamma_1}\left[(k_x^2-k_y^2)\hat{\rho}_x+2\tau k_xk_y\hat{\rho}_y\right]+m_b\hat{\rho}_z, \tag{3}$$

where v is the Fermi velocity, $k_{x,y}$ are the components of the momentum measured relative to the K/K' point, and $\tau=\pm1$ label valley degrees of freedom (K/K'). In the monolayer-like block, the Pauli matrices $\sigma_{x,y,z}$ are denoted on the basis (A_-,B_-), with $A_-=(A_1-A_3)/\sqrt{2}$ and $B_-=(B_1-B_3)/\sqrt{2}$. A_i and B_i are the inequivalent atomic sites of the ith graphene layer. In bilayer-like blocks, the Pauli matrices $\rho_{x,y,z}$ are denoted on the basis (A_+,B_2) with $A_-=(A_1+A_3)/\sqrt{2}$; γ_1 describes hopping matrix element due to the direct nearest interlayer hopping, $m_{s,b}$ are effective sublattice potentials. Compared to Ref. [24], we do not include the mass gap, which can be controlled by an external perpendicular electric field.[13]

Considering the trilayer graphene irradiated by circularly polarized light, the vector potential introduced into the Hamiltonian by substitution $\boldsymbol{k}\to\boldsymbol{k}+e\boldsymbol{A}(t)$ is

$$\boldsymbol{A}(t)=A(\kappa\sin(\omega t),\cos(\omega t)), \tag{4}$$

where ω is the frequency of light, $\kappa=\pm1$ denote right circularity and left circularity, respectively. A is the amplitude of the vector potential. Based on the Floquet theory,[15,25,26], the photon dressed effective Hamiltonian at weak light intensity can be written as

$$\hat{H}^F=\hat{H}+\frac{[\hat{H}_{-1},\hat{H}_1]}{\hbar\omega}+\frac{[\hat{H}_{-2},\hat{H}_2]}{2\hbar\omega}, \tag{5}$$

with

$$\hat{H}_{\pm1} = \frac{\omega}{2\pi}\int_0^{\frac{2\pi}{\omega}}\hat{H}(t)\mathrm{e}^{\pm\mathrm{i}\omega t}\mathrm{d}t, \tag{6}$$

$$\hat{H}_{\pm2} = \frac{\omega}{2\pi}\int_0^{\frac{2\pi}{\omega}}\hat{H}(t)\mathrm{e}^{\pm2\mathrm{i}\omega t}\mathrm{d}t, \tag{7}$$

where $\hat{H}(t)$ is the time-dependent Hamiltonian using the substitution $\boldsymbol{k}\to\boldsymbol{k}+e\boldsymbol{A}(t)$ in Eq. (1) . Straightforward calculations shown the Floquet Hamiltonian as

$$\hat{H}^F=\begin{pmatrix}\hat{H}^F_{\rm slg} & 0\\ 0 & \hat{H}^F_{\rm blg}\end{pmatrix}, \tag{8}$$

where

$$\hat{H}^F_{\rm slg} = \hbar v\,(k_x\hat{\sigma}_x+\tau k_y\hat{\sigma}_y)+\left[m_s+\tau\kappa\Delta^{slg}_\omega\right]\hat{\sigma}_z, \tag{9}$$

$$\hat{H}^F_{\rm blg} = -\frac{\hbar^2v^2}{\gamma_1}\left[(k_x^2-k_y^2)\hat{\rho}_x+2\tau k_xk_y\hat{\rho}_y\right]+\left[m_b+\tau\kappa\Delta^{blg}_\omega\right]\hat{\rho}_z, \tag{10}$$

with

$$\Delta^{slg}_\omega = \frac{v^2}{\hbar\omega}\left(\frac{eA}{\hbar}\right)^2, \tag{11}$$

$$\Delta^{blg}_\omega = \frac{\hbar^4v^4}{\hbar\omega\gamma_1^2}\left(\frac{eA}{\hbar}\right)^2\left[4k^2+\frac{1}{2}\left(\frac{eA}{\hbar}\right)^2\right]. \tag{12}$$

Diagonalizing straightforwardly the Hamiltonian (8), we obtain

$$E^{slg}_\pm = \pm\sqrt{\hbar^2v^2k^2+\left[m_s+\tau\kappa\Delta^{slg}_\omega\right]^2}, \tag{13}$$

$$E^{blg}_\pm = \pm\sqrt{\frac{\hbar^4v^4}{\gamma_1^2}k^4+\left[m_b+\tau\kappa\Delta^{blg}_\omega\right]^2}. \tag{14}$$

Based on Eqs. (13) and (14), we plot the band structures of trilayer graphene in units of $\hbar v=688$ meV for $\tau\kappa=-1$ in Fig. 1. Figure 1(a) shows that the dispersion of trilayer graphene is a combination of the linear dispersion of monolayer graphene and the quadratic relation of bilayer graphene.[4]. The on-site sublattice potential can induce the energy gap in trilayer graphene (see Fig. 1(b) for $m_s=3$ meV, $m_b=8$ meV and $\gamma_1=310$ meV). When considering the circularly polarized light irradiating onto the ABA trilayer graphene sheet, the band structure evolution with light intensity $eA/\hbar$ of 0.186, 0.392, and 0.45 at $\tau\kappa=-1$ are shown in Figs. 1(c)–1(e), respectively. Based on Eqs. (8)–(12), $[\hat{H}_{-1},\hat{H}_1]$ and $[\hat{H}_{-2},\hat{H}_2]$ denote the virtual photon absorption and emission process.[25] They lead to the term $\tau\kappa\Delta^{slg}_\omega\hat{\sigma}_z$ and $\tau\kappa\Delta^{blg}_\omega\hat{\rho}_z$. Thus the light leads to the closing and reopening of energy gap for the fixed sublattice potential, and process of a band gap closing and reopening happen twice. Both the processes are due to the emission and absorption of a single photon and two virtual photons, respectively. Figure 2 shows the energy gap as a function of light intensity $eA/\hbar$. When $\tau\kappa=-1$, the light can lead to the closing and reopening of the energy gap, while the light only amplifies the energy gap for $\tau\kappa=1$.

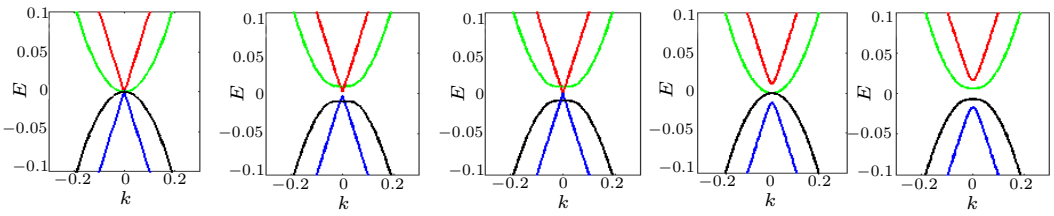


Fig. 1. Band structure of ABA trilayer graphene (a) with and (b) without sublattice potential in units of $\hbar v$. Band structure evolution of ABA trilayer graphene under the irradiation of polarized light with a light intensity $eA/\hbar$ of (c) 0.186, (d) 0.392, and (e) 0.45 at $\tau\kappa=-1$.

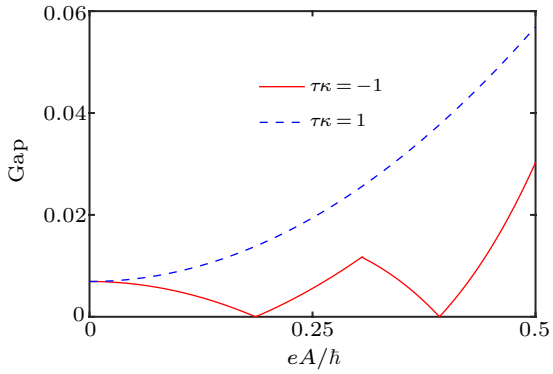


Fig. 2. Energy gap as a function of light intensity $eA/\hbar$. The dashed blue line and the solid red line correspond to $\tau\kappa = 1$ and $\tau\kappa = -1$, respectively.

3. Hall conductivities and Chern numbers

In this section, we investigate anomalous Hall conductivities and Chern numbers in irradiated ABA trilayer graphene. According to the linear response theory, the intrinsic Hall conductance in zero temperature for valley η and circularity κ is given by the integral of the Berry curvature over occupied states[27]

$$\sigma_{xy}^{\tau,\kappa} = \frac{e^2}{\hbar}\sum_n \int_{BZ} \frac{d^2\boldsymbol{k}}{(2\pi)^2}\Omega_n^{\tau,\kappa}, \tag{15}$$

where Ω_n is the momentum-space Berry curvature for the nth band,

$$\Omega_n^{\tau,\kappa}(\boldsymbol{k}) = -\sum_{n'\neq n}\frac{2\mathrm{Im}\langle u_{n\boldsymbol{k}}|v_x|u_{n'\boldsymbol{k}}\rangle\langle u_{n'\boldsymbol{k}}|v_y|u_{n\boldsymbol{k}}\rangle}{(\omega_{n'}-\omega_n)^2}. \tag{16}$$

The summation is taken over all the occupied bands blow the bulk gap, $\omega_n \equiv E_n/\hbar$, and $v_{x(y)} = \partial\hat{H}^F/\partial k_{x(y)}$ is the velocity operator. E_n and $u_{n\boldsymbol{k}}$ are the eigenvalue and eigenfunction of Eq. (8), respectively. In Eq. (8), the monolayer-like block and bilayer-like block are decoupled. Therefore, we can calculate the berry curvature in the two blocks, respectively. Based on Eq. (16), we obtain the berry curvatures for the valence band in the two blocks as follows:

$$\Omega_{\mathrm{slg}}^{\tau,\kappa} = \frac{1}{2}\frac{\hbar^2v^2(m_s+\tau\kappa\Delta_\omega^{slg})}{\left[\hbar^2v^2k^2+(m_s+\tau\kappa\Delta_\omega^{slg})^2\right]^{3/2}}, \tag{17}$$

$$\Omega_{\mathrm{blg}}^{\tau,\kappa} = \frac{\frac{\hbar^4v^4k^2}{\gamma_1^2}\left[m_b+\tau\kappa\Delta_\omega^{slg}\right]}{\left[\frac{\hbar^4v^4}{\gamma_1^2}k^4+(m_b+\tau\kappa\Delta_\omega^{blg})^2\right]^{3/2}}. \tag{18}$$

Figure 3 shows the calculated conductivity $\sigma_{xy} = \sigma_{xy}^{\eta,-1}$ for the two valleys K and K' as a function of Fermi energy E_{F} under the irradiation of left-handed circularly polarized light ($\kappa = -1$) with light intensities (a) $eA/\hbar = 0.1$, (b) $eA/\hbar = 0.2$, and (c) $eA/\hbar = 0.5$. When Fermi energy locates in the energy gap, the anomalous Hall conductivity for valley K ($\eta = 1$) is quantized and unchanged with the increasing light intensity. However, the gap region becomes greater with increasing light intensity. For valley K' ($\eta = -1$), the quantized anomalous Hall conductivities are $2e^2/h$, 0, $-2e^2/h$ with light intensities $eA/\hbar = 0.1$, $eA/\hbar = 0.2$, and $eA/\hbar = 0.5$, respectively. Based on Eqs. (17) and (18), we can find that the changed anomalous Hall conductivities are due to the energy gap changing with the light intensity at different parameters τ and κ. This means that there are topological transitions between anomalous Hall states and Valley Hall states. We analyze Chern numbers in the following paragraphs to confirm the results.

When the fermi energy is in the band gap, the direct correspondence between the Chern number and the Hall conductance is characterized by $\sigma_{xy} = Ce^2/h$,[27] and the Chern number for fixed κ is calculated by

$$C = \frac{1}{2\pi}\sum_{n,\tau}\int_{BZ} d^2\boldsymbol{k}\Omega_n^{\tau,\kappa}. \tag{19}$$

Straightforward calculation shows that the Chern numbers in the two blocks are

$$C_{\mathrm{slg}}^{\tau\kappa} = \mathrm{sgn}\left[m_s+\tau\kappa\frac{v^2}{\hbar\omega}\left(\frac{eA}{\hbar}\right)^2\right], \tag{20}$$

$$C_{\mathrm{blg}}^{\tau\kappa} = \mathrm{sgn}\left[m_b+\tau\kappa\frac{\hbar^4v^4}{2\hbar\omega\gamma_1^2}\left(\frac{eA}{\hbar}\right)^4\right], \tag{21}$$

where sgn represents the sign function. For fixed κ, the Chen number and valley Chern number corresponding to anomalous

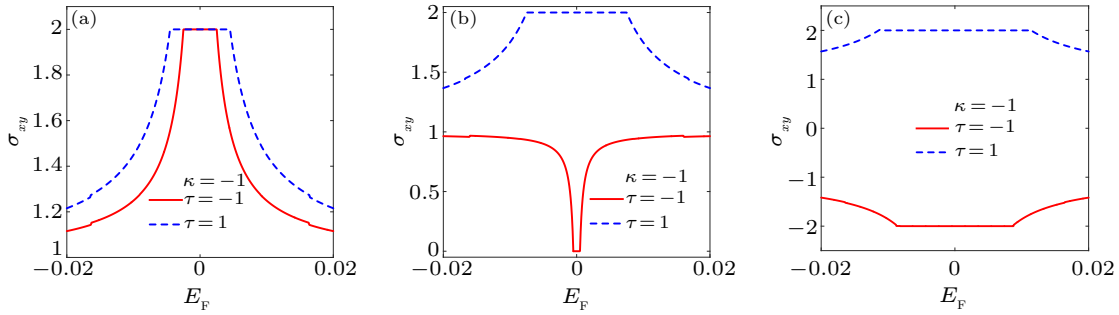


Fig. 3. Anomalous Hall conductivities as a function of Fermi energy E_{F} under the irradiation of left-handed circularly polarized light $\kappa = -1$ in units of e^2/h with light intensities: (a) $eA/\hbar = 0.1$, (b) $eA/\hbar = 0.2$, and (c) $eA/\hbar = 0.5$. Blue-dashed lines and red-solid lines denote Hall conductivities in K and K', respectively.

Hall and valley Hall states are

$$C_{\mathrm{AH}} = \sum_{\tau} C_{\mathrm{slg}}^{\tau\kappa} + C_{\mathrm{blg}}^{\tau\kappa}, \tag{22}$$

$$C_{\mathrm{VH}} = \sum_{\tau} \tau[C_{\mathrm{slg}}^{\tau\kappa} + C_{\mathrm{blg}}^{\tau\kappa}]. \tag{23}$$

In Fig. 4, we plot C_{AH} and C_{VH} versus light intensity A for $\kappa = -1$. This is consistent with the results shown in Fig. 2. Before the first band gap closing and reopening, the Chern numbers of the two valley sectors in two blocks take the same value 1. As a whole, the system shows a quantized anomalous Hall state ($C_{\mathrm{AH}} = 4$ and $C_{\mathrm{VH}} = 0$). With increasing A, the band gap closing and reopening occur in monolayer-like block, and the corresponding Chern numbers of the two valley sectors take the values 1 and -1, respectively. The Chern numbers in the bilayer-like block keep unchanged. Therefore, the system shows coexistence of a quantized anomalous Hall state and a valley Hall state ($C_{\mathrm{AH}} = 2$ and $C_{\mathrm{VH}} = 2$). After the band gap closing and reopening in the bilayer-like block, the Chern numbers of the two valley sectors in the two blocks take the values of 1 and -1, respectively. The system shows a quantized valley Hall state ($C_{\mathrm{AH}} = 0$ and $C_{\mathrm{VH}} = 4$). Consequently, the sign of the Chern number is changed only in one valley but remains the same in the other valley in the two blocks. Hence, we can realize an anomalous Hall state to the valley Hall state topological phase transition.

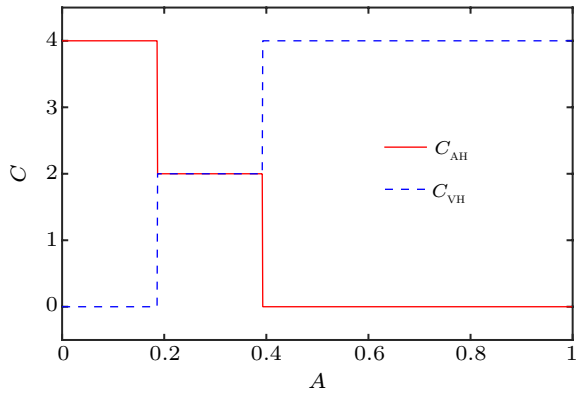


Fig. 4. Chern number as a function of A for $\kappa = -1$. The solid red line and the dashed blue line denote the Chen number and the valley Chern number corresponding to anomalous Hall and valley Hall states, respectively.

4. Conclusion and summary

To conclude, we have analyzed Hall conductivities and Chern numbers of ABA trilayer graphene under the application of a circularly polarized light. We have employed the Floquet theory to obtain the effective Hamiltonian with a circularly polarized light in high-frequency regime. We find a process of band gap closing and reopening due to irradiation of light, and it happens twice. The study on the corresponding Chern numbers confirms the light-induced topological phase transition between anomalous Hall state and valley Hall state. The interplay between effective sublattice potential and light-induced circularity-dependent effective potential is responsible for the topological phase transition.

References

[1] Novoselov K S, Geim A K, Morozov S V, Jiang D, Zhang Y, Dubonos S V, Grigorieva I V and Firsov A A 2004 *Science* **306** 666
[2] Castro Neto A H, Guinea F, Peres N M R, Novoselov K S and Geim A K 2009 *Rev. Mod. Phys.* **81** 109
[3] Taychatanapat T, Watanabe K, Taniguchi T and Jarillo-Herrero P 2011 *Nat. Phys.* **7** 621
[4] Bao W, Jing L, Velasco J, Lee Y, Liu G, Tran D, Standley B, Aykol M, Cronin S B, Smirnov D, Koshino M, McCann E, Bockrath M and Lau C N 2011 *Nat. Phys.* **7** 948
[5] Lui C H, Li Z, Mak K F, Cappelluti E and Heinz T F 2011 *Nat. Phys.* **7** 944
[6] Lui C H, Ye Z, Keiser C, Barros E B and He R 2015 *Appl. Rev. Lett.* **106** 041904
[7] Asakawa Y, Masubuchi S, Inoue N, Morikawa S, Watanabe K, Taniguchi T and Machida T 2017 *Phys. Rev. Lett.* **119** 186802
[8] Scherer M M, Uebelacker S, Scherer D D and Honerkamp C 2012 *Phys. Rev. B* **86** 155415
[9] Zhang L, Zhang Y, Camacho J, Khodas M and Zaliznyak I 2011 *Nat. Phys.* **7** 953
[10] Jung J and MacDonald A H 2013 *Phys. Rev. B* **88** 075408
[11] Kumar A, Escoffier W, Poumirol J M, Faugeras C, Arovas D P, Fogler M M, Guinea F, Roche S, Goiran M and Raquet B 2011 *Phys. Rev. Lett.* **107** 126806
[12] Stepanov P, Barlas Y, Espiritu T, Che S, Watanabe K, Taniguchi T, Smirnov D and Lau C N 2016 *Phys. Rev. Lett.* **117** 076807
[13] Barlas Y 2018 *Phys. Rev. Lett.* **121** 066602
[14] Chittari B L, Chen G, Zhang Y, Wang F and Jung J 2019 *Phys. Rev. Lett.* **122** 016401
[15] Oka T and Aoki H 2009 *Phys. Rev. B* **79** 081406
[16] Syzranov S V, Rodionov Ya I, Kugel K I and Nori F 2013 *Phys. Rev. B* **88** 241112
[17] Perez-Piskunow P M, Usaj G, Balseiro C A and Foa Torres L E F 2014 2014 *Phys. Rev. B* **89** 121401
[18] Glazov M M and Ganichev S D 101 *Phys. Rep.* **535** 101
[19] Kibis O V, Dini K, Iorsh I V and Shelykh I A 2017 2017 *Phys. Rev. B* **95** 125401
[20] Usaj G, Perez-Piskunow P M, Foa Torres L E F and Balseiro C A 2014 *Phys. Rev. B* **90** 115423
[21] Li S, Liu C C and Yao Y 2018 *New J. Phys.* **20** 033025
[22] Xu D H, Yuan J, Yao Z J, Zhou Y, Gao J H and Zhang F C 2012 *Phys. Rev. B* **86** 201404
[23] Zhu G B and Zhang P 2013 *Chin. Phys. B* **22** 017303
[24] Serbyn M and Abanin D A 2013 *Phys. Rev. B* **87** 115422
[25] Kitagawa T, Oka T, Brataas A, Fu L and Demler E 2011 *Phys. Rev. B* **84** 235108
[26] Lindner N H, Refael G and Galitski V 2011 *Nat. Phys.* **7** 490
[27] Thouless D J, Kohmoto M, Nightingale M P and den Nijs M 1982 *Phys. Rev. Lett.* **49** 405